

Biotechnology Research Center and Faculty of Advanced Medical Science<sup>1</sup>, Tabriz University of Medical Sciences, Tabriz; Zanzan Pharmaceutical Nanotechnology Research Center and Department of Pharmaceutics<sup>2</sup>, Faculty of Pharmacy, Zanzan University of medical Sciences, Zanzan; Students' Research Committee and Faculty of Pharmacy<sup>3</sup>; Department of Oral and Maxillofacial Pathology<sup>4</sup>, Faculty of Dentistry; Research Center for Pharmaceutical Nanotechnology and Faculty of Advanced Medical Science<sup>5</sup>; Drug Applied Research Center<sup>6</sup>, Tabriz University of Medical Sciences, Tabriz, Iran

## Enhanced skin penetration of lidocaine through encapsulation into nanoethosomes and nanostructured lipid carriers: a comparative study

S. BABAEI<sup>1</sup>, S. GHANBARZADEH<sup>2</sup>, Z. M. ADIB<sup>3</sup>, M. KOUHSOLTANI<sup>4</sup>, S. DAVARAN<sup>5</sup>, H. HAMISHEHKAR<sup>6</sup>

Received September 25, 2015, accepted January 2, 2016

Hamed Hamishehkar, Drug Applied Research Center, Tabriz University of Medical Sciences, Golgasht Ave, Tabriz, Iran

Hamishehkarh@tbzmed.ac.ir

Pharmazie 71: 247–251 (2016)

doi: 10.1691/ph.2016.5158

Lipid based nanoparticles have become a major research object in topical drug delivery to enable drugs to pass the stratum corneum and reach the desired skin layer. The present investigation deals with the encapsulation of lidocaine into nanostructured lipid carriers (NLCs) and nanoethosomes for improving its dermal delivery and consequently local anesthetic efficacy. Concurrently these two topical delivery systems were compared. Lidocaine-loaded NLCs and nanoethosomes were characterized by various techniques and used for an *in vitro* skin penetration study using excised rat skin and Franz diffusion cells. The nanoparticles were tracked in the skin by following the Rhodamine-labeled nanocarriers under fluorescent microscopy. Optimized lidocaine-loaded NLCs (size 96 nm, zeta potential -13.7 mV, encapsulation efficiency (EE) % 69.86% and loading capacity (LC) % 10.47%) and nanoethosomes (size 105.4 nm, zeta potential -33.6 mV, EE 40.14% and LC 8.02%) were chosen for a skin drug delivery study. Higher skin drug deposition of NLCs and nanoethosomal formulations compared to lidocaine hydroalcoholic solution represented a better localization of the drug in the skin. NLC formulation showed the lowest entered drug in the receptor phase of Franz diffusion cell in comparison with nanoethosomes and hydroalcoholic solution confirming the highest skin accumulation of drug. Both colloidal systems showed superiority over the drug solution for dermal delivery of lidocaine, however, NLC exhibited more promising characteristics than nanoethosomes regarding drug loading and skin targeted delivery.

### 1. Introduction

Drug delivery to or through the skin shows both opportunities and difficulties due to skin structure, physiology, and barrier properties. New topical drug delivery systems such as particulate carriers help the drug to pass the stratum corneum and reach the preferred site of action (Babaie et al. 2015; Hamishehkar et al. 2013). A number of carrier systems like microemulsions, liposomes and lipid based nanoparticles have been investigated for dermal delivery of drugs. These systems may enhance drug permeation in skin, increase duration of local action, and prevent systemic absorption of drugs thereby reducing the associated side effects of drugs (Allen et al. 2013; Dolatabadi et al. 2015; Ghanbarzadeh et al. 2014; Javadzadeh and Hamishehkar 2011). In any anesthetic topical application, the drug should penetrate the stratum corneum (SC) and desensitize the underlying pain receptors within the skin (Halperin et al. 1989; Naganawa et al. 2015). Since epidermal lipids are found in high amounts within the penetration barrier, lipid carriers such as liposomes, solid lipid nanoparticles (SLN) and Nanostructured lipid carriers (NLC) appear promising carriers by attaching themselves to the skin surface and allowing lipid exchange between the outermost layers of the stratum corneum and the carrier (Gainza et al. 2015; Morales et al. 2015; Nagarsenker et al. 2015). NLCs are the second generation of lipid nanoparticles in which the solid lipid of SLNs are partially substituted by oils. This provides increased drug loading in the carrier system, better permeability into the dermal layer and satisfactory physical stability (Gönüllü et al. 2015; Pradhan et al. 2015). Ethosomes are other novel lipid carriers which are composed of phospholipid and high ethanol concentration (20–40%). High ethanol content of ethosomes results in being much smaller than liposomes, enhances

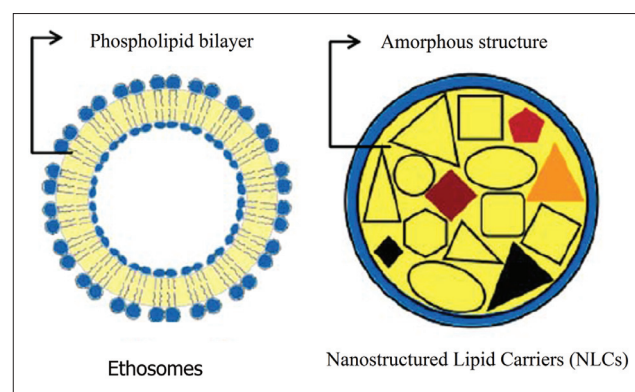


Fig. 1: Schematic image of ethosomes and nanostructured lipid carriers (NLC)

solubility of more lipophilic drugs and causes to be more flexible than liposomes. Besides these, disruption of intercellular lipid structure of stratum corneum by the phospholipids, improves drugs permeation (Ahad et al. 2013). Deep anesthesia in skin is useful to relieve pain in procedures involving the skin such as venipuncture, lumbar puncture, skin biopsy, and removal of hair in hirsutism (Ji et al. 2015; Jung et al. 2015). An optimized formulation of lidocaine is expected to have a fast onset and long duration of deep local anesthesia with reduced systemic absorption and side effects. This publication describes the preparation, characterization and comparison of nanoethosomal and NLC formulations for dermal delivery of lidocaine. Both drug delivery systems were also compared in the point of drug encapsulation and dermal delivery.

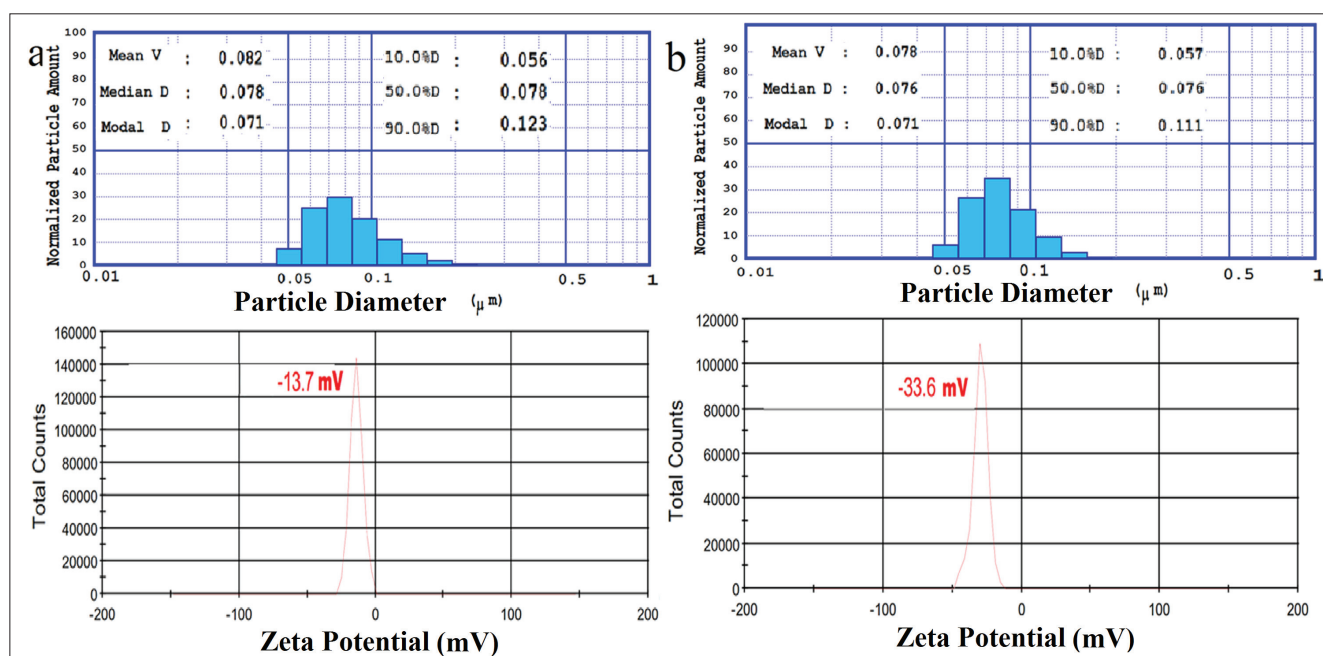


Fig. 2: Particle size distributions (top) and zeta potential values (down) of optimized Lidocaine-loaded NLC (a) and nanoethosomal (b) formulations.

## 2. Investigations, results and discussion

### 2.1. Characterization of lidocaine-loaded NLC and nanoethosomes

Both types of prepared nanoparticles were almost in the same size around 80 nm with narrow size distribution (Fig. 2). This provided a suitable condition for comparative investigation of dermal delivery of lipid particulate (NLC) and lipid vesicular (ethosome) drug carriers. Entrapment efficiency (EE, %) and loading capacity (LC, %) of optimized NLC and nanoethosomal formulations were  $69.86 \pm 3.45$  %,  $10.47 \pm 1.53$  % and  $40.14 \pm 4.10$  %,  $8.02 \pm 0.9$  %, respectively. The comparison of LC values indicated that NLC provided more capacity for drug entrapment than nanoethosomes.

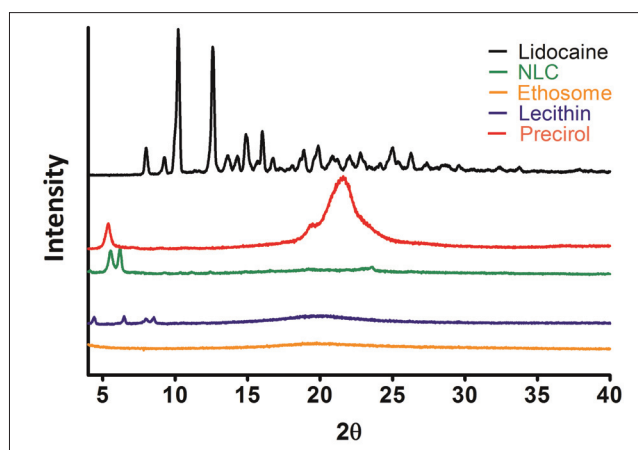


Fig. 3: The X-ray diffractions pattern of Lidocaine, Precirol®, Phosphatidylcholine, optimized Lidocaine-loaded NLC and nanoethosomal formulations.

Contrary to SLNs being prepared from solid lipids, the NLCs are fabricated with blends of solid lipids and liquid lipids. The solubility of drugs in oils is usually much higher than in solid lipids. Therefore, the higher loading capacity could be achieved by the development of NLC. Fig. 2b illustrated that nanoethosomes (-33.6 mV) had higher zeta potential values than NLCs (-13.7 mV). Zeta potential values more negative than -30 mV are generally considered to represent adequate reciprocal repulsion to guarantee the stability of a dispersion, as is well-known from colloidal science (Freitas and Müller 1998; Rodríguez-Valverde et al. 2003). Therefore, nanoethosomes may provide a more stable colloidal drug

delivery system for lidocaine than NLCs. On the other hand, the poloxamer used in the formulation of NLC makes a sufficient steric stability for nanoparticles available (Alam et al. 2015). The diffraction pattern of lidocaine analyzed by a X-ray diffraction method exhibited several sharp peaks indicating the crystalline nature of lidocaine (Fig. 3). The characteristic main peaks for lidocaine were absent in the XRD pattern of NLC and nanoethosomal formulations suggesting that lidocaine was uniformly and molecularly distributed in the lipid matrix of NLCs and lipid bilayers of nanoethosomes. This finding helps the interpretation of observed high LC (around 10%) for both systems. Diffraction pattern of the lipids of both systems (Precirol® in NLC and phosphatidylcholine in nanoethosomes) was much weaker than that of bulk lipid. It shows that Precirol® and phosphatidylcholine in lidocaine-loaded NLC and nanoethosomes were partially formed in the less-ordered crystals. Admixture of liquid with solid lipids leads to the creation of a less ordered inner structure (amorphous state). Thus, the drug molecules can be accommodated in between lipid layers and/or fatty acid chains. With this approach, drug loading is increased and expulsion during storage time is also reduced (Hamishehkar et al. 2015a).

### 2.2. In vitro drug permeation and skin deposition studies

The cumulative percentage of permeated lidocaine from NLC and nanoethosomal formulations and hydroalcoholic solution through excised rat skin was investigated using Franz diffusion cell for a period of 24 h. As shown in Fig. 4, the ratio of drug penetrated through stratum corneum was slightly improved (around 10%) by nanoparticulate drug carriers. This improvement was not statistically significant in the case of NLC ( $p > 0.05$ ) which might correspond to the characteristics of lidocaine (molecular weight = 234.34 and Log P = 2.6) which favour skin penetration ( $MW < 500$  and Log P 1-4) (Cronin et al. 1999; Kang et al. 2007). However, the drug penetrated through SC from hydroalcoholic formulation and lipid based nanocarriers showed two different destinies. The former system concluded around 14% of drug diffusion to the receiver compartment of Franz cell. However, nanoethosomes and NLCs directed only 2.5% and 0.2% of lidocaine to the receiver compartment of the Franz cell. The receiver compartment of the Franz cell is a simulator for drug systemic absorption. Therefore, lipid based nanoparticles especially NLCs could be successfully applied for topical drug therapy with avoiding systemic drug absorption. This would be ideal for delivery of drugs such as analgesics especially for those causing systemic adverse effects such as lidocaine.

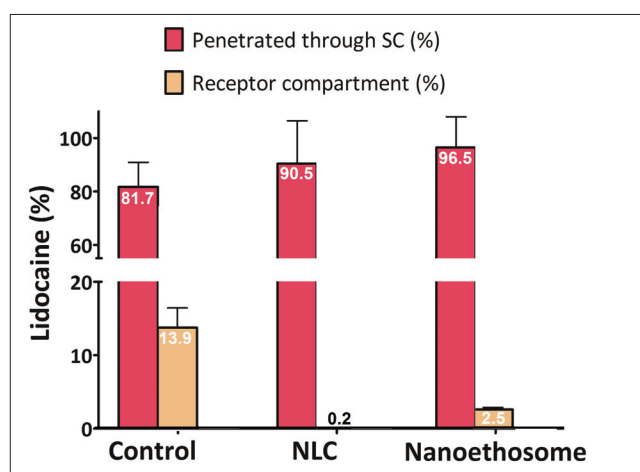


Fig. 4: Deposited lidocaine in the skin, passed lidocaine through the stratum corneum from Lidocaine-loaded NLC nanoethosomal formulations and hydro alcoholic solution, determined *in vitro* on exercised rat skin by Franz diffusion cells.

### 2.3. *In vivo* experiments

Figure 5 shows that although both nanocarriers penetrated into the skin, nanoethosomes mostly remained in the stratum corneum but NLC completely passed it to the lower layers of epidermis and somehow in the deeper parts of dermis. This might be attributed the vesicular structure of nanoethosomes and the solid matrix construction of NLCs. The vesicular structure disrupted easily in the stratum corneum while rigid structure of NLC preserved the entrapped payload and carried it to the deeper layers of skin. Figure 5 indicates that the follicular pathway plays the main role in the penetration of both nanoparticulate carriers into skin.

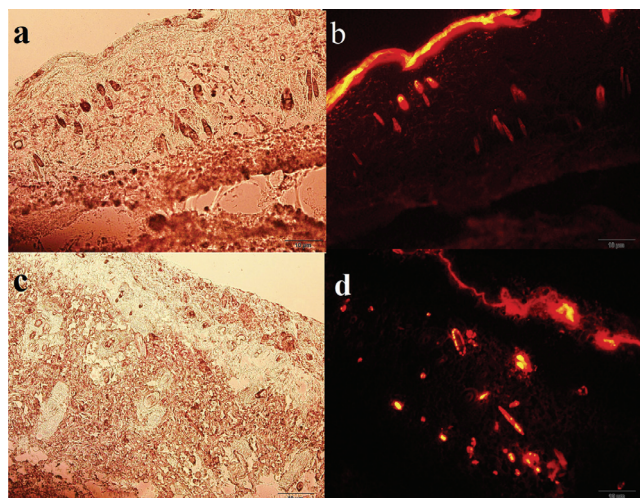


Fig. 5: Rhodamine B penetration into rat skin: staining of rat skin following the application of 0.001% Rhodamine B-loaded NLC (a: light microscopic image, b: fluorescent microscopic image) and nanoethosomal (c: light microscopic image, d: fluorescent microscopic image) formulation for 0.5 h.

### 2.4. Conclusion

Improving the efficacy of topical therapy by lipid based nanoparticulate carrier systems has attracted increasing interest. The present work is on the preparation and comparison of lidocaine-loaded NLC and nanoethosomal formulations to improve lidocaine permeation through the stratum corneum and deposition in the skin. Both NLC and nanoethosomal formulations increased lidocaine permeation and skin deposition. An advantage of lipid based nanoparticulate drug carriers was that they achieved higher skin deposition and lower systemic drug absorption. NLC led to better skin drug deposition than nanoethosomes. In conclusion, results

of the present study indicated that both lipid based nanoparticles investigated especially NLCs are promising carriers for improving the targeted delivery of lidocaine to enhance drug onset of action, increase its duration of action and reduce drug systemic absorption.

## 3. Experimental

### 3.1. Materials

Lidocaine was obtained from Darou Pakhsh Pharm. Chem. Co. (Tehran, Iran). Glycerol palmitostearate (Precirol ATO-5<sup>®</sup>) was prepared from Gattefossé Company (Lyon, France). Cholesterol and lecithin were prepared from Merck Company (Germany). Poloxamer<sup>®</sup> 407 was supplied from Sigma-Aldrich Company (Darmstadt, Germany). Chloroform (Dae-Junge, Korea), ethanol (Merck, Germany) and diethyl ether (KianKaveh Pharmaceutical and Chemical Company, Tehran, Iran) were used as received. Rhodamine B was obtained from Merck Chemicals Company (Darmstadt, Germany).

### 3.2. Preparation of lidocaine-loaded NLC and nanoethosomes

NLC were prepared by the hot melt homogenization method as described previously (Hamishehkar et al. 2015b). Precirol ATO-5<sup>®</sup> and Miglyol (containing lidocaine) were melted at about 85 °C. Subsequently, the aqueous phase was prepared by dissolving Poloxamer<sup>®</sup> 407 in double-distilled water and heating to the same temperature as the oil phase. The aqueous phase was added dropwise to the oil phase under stirring at 20000 rpm by a homogenizer (DIAX 900, Heidolph, Germany), keeping the temperature at 85 °C and allowing the hot formulation to cool down at room temperature. Each formulation was prepared and characterized in triplicate. In the present study, nanoethosomes were prepared by a modified ethanol injection method. Briefly, phosphatidylcholine, cholesterol, and Lidocaine were dissolved in ethanol and injected slowly into the aqueous medium under mixing by homogenizer (Ghanbarzadeh and Arami 2013; Ghanbarzadeh et al. 2013).

### 3.3. Characterization of lidocaine-loaded NLC and ethosomes

#### 3.3.1. Particle size determination

Particle size and zeta potential were analyzed by a laser diffraction method using a particle size analyzer (SALD 2101, Shimadzu, Japan) which provides information about the mean diameter of the bulk population based on the volume mean diameter (VMD). The laser diffraction method irradiates samples with laser light and detects the changes in intensities, which vary depending on the angle of the diffracted and scattered light. It then uses calculations to determine the particle size distribution. The SALD-2101 uses a UV laser light source and a contiguous wide angle scattered light detection system that allow observing not only primary particles but also aggregates and contaminants, ranging from the nano region to several hundred micrometers, simultaneously and in real time. Span value was used as a size distribution index and calculated according to the following equation:

$$Span = \frac{D_{90\%} - D_{10\%}}{D_{50\%}}$$

where  $D_{10\%}$ ,  $D_{50\%}$  and  $D_{90\%}$  indicate the percentage of particles having 10, 50 and 90% of the diameter equal to or lower than the given value (Rasaei et al. 2015). Prior to measurement, formulations samples were diluted with double-distilled water. Each sample was measured in triplicate.

#### 3.3.2. Determination of zeta potential

The zeta potential of samples were measured by a laser-scattering technique (Zetasizer Nano ZS90; Malvern Instruments, Malvern, UK) with a He-Ne laser (633 nm) and 90° collecting optics at 25 °C. The nanocarriers were diluted 100-fold with double-distilled water before the examination. The measurement was repeated three times per sample for three samples and the zeta potential values were calculated according to the Smolochowski equation.

#### 3.3.3. Entrapment efficiency (EE) and loading capacity (LC)

The EE (%) and LC (%) were expressed as the percentage of entrapped drug to the added drug or to the used lipid, respectively. Entrapment efficiency was determined by first separation of the un-entrapped drug by the centrifugation method using of Amicon<sup>®</sup> Ultra-15 with molecular weight cutoff of 100 kDa (Millipore, Germany) tube. The formulation was added to the upper chamber of the Amicon<sup>®</sup> tube and then the tube was centrifuged (Sigma 3K30, Germany) at 5000 rpm for 5 min. The clear solution in the bottom of Amicon<sup>®</sup> tube was used for Lidocaine determination using a validated HPLC and mathematically calculated according to the following equations:

$$EE (\%) = \frac{W_{(Initial\ drug)} - W_{(Free\ drug)}}{W_{(Initial\ drug)}} \times 100$$

$$LC (\%) = \frac{W_{(Entrapped\ drug)}}{W_{(Total\ lipid)}} \times 100$$

where  $W_{(\text{initial drug})}$  is the amount of initial drug used and  $W_{(\text{free drug})}$  is the amount of free drug detected in the lower chamber of Amicon® tube after centrifugation of the SLN formulations. Accordingly,  $W_{(\text{entrapped drug})}$  is the amount of loaded drug and  $W_{(\text{total lipid})}$  is the amount of the lipid used in the preparation process (Ghaderi et al. 2015). The formulations in the upper chamber of the Amicon® tube were rinsed five times by hydro alcoholic (50%) solution to eliminate unloaded Lidocaine. These rinsed formulations were used for the rest experiments (Hooresfand et al., 2015).

### 3.3.4. HPLC analysis of lidocaine

Lidocaine was analyzed using a validated reversed-phase HPLC method by a Knauer HPLC apparatus (Germany), consisting of a sensitive variable wavelength ultraviolet detector (set at  $\lambda_{\text{max}} = 254 \text{ nm}$ ) and a VP-ODS column (C18, 10  $\mu\text{m}$ , 4.6  $\times$  250 mm). The samples were eluted using a mobile phase consisting of phosphate buffer: acetonitrile (65:35 v/v) at a flow rate of 1 mL/min. The calibration curve was linear in the concentration range of 1–50  $\mu\text{g/mL}$  ( $r^2 = 0.9998$ ). No interference from the formulation components or skin tissue was observed. The samples were also found to be stable during the study period. The mobile phase was filtered through a 0.45  $\mu\text{m}$  cellulose acetate filter under vacuum and degassed by sonication (Starsonic 35, Italy) in order to protect the column.

### 3.3.5. X-ray diffraction (XRD) studies

In order to assess the effect of NLC and nanoethosome preparation process on crystallographic patterns of lidocaine and lipids, XRD analysis was performed using an X-ray diffractometer (D-5000, Siemen, Germany, 2° to 40°) to assess the crystalline structures of lidocaine, Precirol®, Poloxamer®, phosphatidylcholine, and vacuum-dried (Binder, Germany) powder of optimized NLC and nanoethosomal formulations. The diffraction pattern was measured using a Cu-K $\alpha$  radiation source (30 mA and 40 kV).

### 3.4. In vitro skin permeation and drug deposition studies

Male Wistar rats (weighing 200–250 g) were obtained from Pasteur Institute (Tehran, Iran), housed in animal facilities of the Drug Applied Research Center (Tabriz University of Medical Science) and used for skin permeation and drug deposition studies. All animal experiments were conducted according to the Guide for Care and Use of Laboratory Animals of Tabriz University of Medical Sciences, Tabriz, Iran (National Institutes of Health Publication No 85-23, revised 1985). The abdominal full thickness skin was shaved using an electric razor after sacrificing with excess ether inhalation. The skin was washed and subcutaneous fat was carefully removed. Subsequently, to remove extraneous debris and leachable enzymes, the dermal side of the skin was in contact with a saline solution for 12 h before starting the *in vitro* skin penetration study. The skins were mounted on the Franz-type diffusion cells with an available diffusion area of 3.14  $\text{cm}^2$  and the receptor compartment volume of 25  $\text{cm}^3$ . The stratum corneum was faced to the donor compartment of the Franz-type diffusion cells (HDT6, Erweka, Germany). Twenty four milliliter of acetate buffer solution (pH 7.4 and 37 °C) was used as the receptor medium (stirred with Teflon-coated magnetic stirring bars at 700 rpm) and 200  $\mu\text{L}$  of the formulation was applied on the skin surface in the donor compartment. The donor chamber and the sampling port were covered by parafilm to prevent evaporation during the study. Samples of 250  $\mu\text{L}$  were withdrawn from the receptor compartment after 24 h (Hamishehkar et al. 2015b). At the end of the experiment, the amounts of drug remaining on the skin and the drug concentration in the skin (frozen with liquid nitrogen and then cut and grinded into small species) were quantified by extraction into methanol followed by HPLC analysis. The amount of drug in the samples withdrawn from the receptor compartment was also assayed with HPLC apparatus as well. Each set of experiments was performed in three diffusion cells and was repeated three times in different days.

### 3.5. In vivo studies

Fluorescence measurement allows to follow the distribution of dyes in skin and therefore, lets the study of the carrier effects and selection of the most suitable system. Rhodamine B labeled lidocaine-loaded NLC and nanoethosomal formulations were prepared (dye content = 0.001%) in the same concentration to study the penetration behavior of NLC and nanoethosomal formulations by an imaging technique (Raphael et al. 2013; Subongkot et al. 2013; Trauer et al. 2014). The unloaded Rhodamine B was removed from the formulation by dialysis through cellulose acetate membrane (cut off molecular weight 12 kDa, Sigma USA). Each formulation (200  $\mu\text{L}$ ) was applied on the skin surface and after 0.5 h exposure, rats were sacrificed with excess ether inhalation and then the skin was cut into 1.5 $\times$ 1.5  $\text{cm}^2$  pieces and rinsed with distilled water. An aqueous solution of Rhodamine B was used as control. Skins were cut into vertical slices with 15  $\mu\text{m}$  thickness by a freeze microtome (Kryomat 1700, Leitz, Germany) and slices were stored at +4 °C and analyzed within 24 h. The skin slices were investigated under both normal light and fluorescence microscopes (BX50, Olympus, Japan). The images were taken from normal light and fluorescence microscope of the same area and the dye distribution in the skin was evaluated qualitatively (Hamishehkar et al. 2015a).

### 3.6. Statistical analysis

All of the skin permeation experiments were repeated in triplicate and data were expressed as a mean value  $\pm$  standard deviation (SD). Statistical analysis was performed using a one-way analysis of variance (ANOVA) with multiple comparisons between deposition data using a Tukey honest significant difference (HSD) test using SPSS software (version 13.0, Chicago, IL, USA). A P value <0.05 was considered statistically significant.

**Acknowledgments:** This paper was extracted from M.Sc. thesis (No. 92/2-6/3) that was submitted to the Faculty of Advanced Medical Science of Tabriz University of Medical Sciences and financially supported by Drug Applied Research Center of the same university.

**Conflict of interest:** The authors report no conflicts of interest.

### References

- Ahad A, Aqil M, Kohli K, Sultana Y, Mujeeb M (2013) Enhanced transdermal delivery of an anti-hypertensive agent via nanoethosomes: Statistical optimization, characterization and pharmacokinetic assessment. *Int J Pharm* 443: 26-38.
- Alam T, Pandit J, Vohora D, Aqil M, Ali A, Sultana Y (2015) Optimization of nanostructured lipid carriers of lamotrigine for brain delivery: *in vitro* characterization and *in vivo* efficacy in epilepsy. *Expert Opin Drug Del* 12: 181-194.
- Allen TM, Cullis PR (2013) Liposomal drug delivery systems: from concept to clinical applications. *Adv Drug Del Rev* 65: 36-48.
- Babaie S, Ghanbarzadeh S, Davaran S, Kouhsoltani M, Hamishehkar H (2015) Nanoethosomes for dermal delivery of lidocaine. *Adv Pharm Bull* 5: 549-556.
- Cronin M, Dearden J, Moss G, Murray-Dickson G (1999) Investigation of the mechanism of flux across human skin in vitro by quantitative structure-permeability relationships. *Eur J Pharm Sci* 7: 325-330.
- Dolatabadi JEN, Valizadeh H, Hamishehkar H (2015) Solid Lipid Nanoparticles as efficient drug and gene delivery systems: recent breakthroughs. *Adv Pharm Bull* 5: 151-159.
- Freitas C, Müller RH (1998) Effect of light and temperature on zeta potential and physical stability in solid lipid nanoparticle (SLN™) dispersions. *Int J Pharm* 168: 221-229.
- Gainza G, Chu W, Guy R, Pedraz J, Hernandez R, Delgado-Charro B, Igartua M (2015) Development and *in vitro* evaluation of lipid nanoparticle-based dressings for topical treatment of chronic wounds. *Int J Pharm* 490: 404-411.
- Ghaderi S, Ghanbarzadeh S, Hamishehkar H (2015) Evaluation of different methods to produce nanoparticle containing gammaoryzanol for potential use in food fortification. *Pharm Sci* 20: 130-134.
- Ghanbarzadeh S, Arami S (2013) Formulation and evaluation of piroxicam transferosomal gel: an approach for penetration enhancement. *J Drug Deliv Sci Technol* 23: 587-590.
- Ghanbarzadeh S, Khorrami A, Arami S (2014) Preparation of optimized Naproxen nano liposomes using response surface methodology. *J Pharm Invest* 44: 33-39.
- Ghanbarzadeh S, Valizadeh H, Zakeri-Milani P (2014) Sirolimus Nano Liposomes / Optimization of sirolimus nano liposomes prepared by modified ethanol injection method using response surface methodology. *Pharm Ind* 75: 1-4.
- Gönüllü Ü, Üner M, Yener G, Karaman EF, Aydoğmuş Z (2015) Formulation and characterization of solid lipid nanoparticles, nanostructured lipid carriers and nanoemulsion of lornoxicam for transdermal delivery. *Acta Pharm* 65: 1-13.
- Halperin DL, Koren G, Attias D, Pellegrini E, Greenberg ML, Wyss M (1989) Topical skin anesthesia for venous, subcutaneous drug reservoir and lumbar punctures in children. *Pediatrics* 84: 281-284.
- Hamishehkar H, Ghanbarzadeh S, Sepهران S, Javadzadeh Y, Adib ZM, Kouhsoltani M (2015a) Histological assessment of follicular delivery of flutamide by solid lipid nanoparticles: potential tool for the treatment of androgenic alopecia. *Drug Dev Ind Pharm*, in Press, doi: 10.3109/03639045.2015.1062896.
- Hamishehkar H, Rahimpour Y, Kouhsoltani M (2013) Niosomes as a propitious carrier for topical drug delivery. *Expert Opin Drug Del* 10: 261-272.
- Hamishehkar H, Shokri J, Fallahi S, Jahangiri A, Ghanbarzadeh S, Kouhsoltani M (2015b) Histopathological evaluation of caffeine-loaded solid lipid nanoparticles in efficient treatment of cellulite. *Drug Dev Ind Pharm* 41: 1640-1646.
- Hooresfand Z, Ghanbarzadeh S, Hamishehkar H (2015) Preparation and characterization of rutin-loaded nanophytosomes. *Pharm Sci* 21: 145-151.
- Javadzadeh Y, Hamishehkar H (2011) Enhancing percutaneous delivery of methotrexate using different types of surfactants. *Colloids Surf B Biointerfaces* 82: 422-426.
- Ji Y, Guo L, Zhang Y, Liu Y (2015) Comparison of topical anesthesia and subcutaneous infiltration anesthesia with regard to effect of plasma skin regeneration system. *J Cosmet Laser Ther* 2015: 1-5.
- Jung YS, Han Y-R, Choi E-S, Kim B-G, Park H-P, Hwang J-W, Yeon YT (2015) The optimal anesthetic depth for interventional neuroradiology: comparisons between light anesthesia and deep anesthesia. *Korean journal of anesthesiology*. 68: 148-152.
- Kang L, Yap C, Lim P, Chen Y, Ho P, Chan YW, Wong GP, Chan SY (2007) Formulation development of transdermal dosage forms: Quantitative structure-activity relationship model for predicting activities of terpenes that enhance drug penetration through human skin. *J. Control Release* 120:211-219.
- Morales JO, Valdés K, Morales J, Oyarzun-Ampuero F (2010) Lipid nanoparticles for the topical delivery of retinoids and derivatives. *Nanomedicine* 10: 253-269.
- Naganawa T, Baad-Hansen L, Ando T, Svensson P (2015) Influence of topical application of capsaicin, menthol and local anesthetics on intraoral somatosensory sensitivity in healthy subjects: temporal and spatial aspects. *Exp Brain Res* 233: 1189-1199.
- Nagarsenker MS, Jain AS, Shah SM (2015) Functionalized Lipid Particulates in Targeted Drug Delivery. *Targeted Drug Delivery: Concepts and Design*: Springer. p 411-431.
- Pradhan M, Singh D, Murthy SN, Singh MR (2015) Design, characterization and skin permeating potential of fluocinonide acetone loaded nanostructured lipid carriers for topical treatment of psoriasis. *Steroids* 101: 56-63.
- Raphael AP, Meliga SC, Chen X, Fernando GJ, Flaim C, Kendall MA (2013) Depth-resolved characterization of diffusion properties within and across minimally-perturbed skin layers. *J Control Release* 166: 87-94.

---

## ORIGINAL ARTICLES

- Rasae S, Ghanbarzadeh S, Mohammadi M, Hamishehkar H (2015) Nano phyto-somes of quercetin: a promising formulation for fortification of food products with antioxidants. *Pharm Sci* 20: 96-101.
- Rodriguez-Valverde M, Cabrerizo-Vilchez M, Paez-Duenas A, Hidalgo-Alvarez R (2003) Stability of highly charged particles: bitumen-in-water dispersions. *Colloids Surf Physicochem Eng Aspects* 222: 233-251.
- Subongkot T, Wonglertnirant N, Songprakhon P, Rojanarata T, Opanasopit P, Ngawhirunpat T (2013) Visualization of ultradeformable liposomes penetration pathways and their skin interaction by confocal laser scanning microscopy. *Int J Pharm* 441: 151-161.
- Trauer S, Richter H, Kuntsche J, Büttemeyer R, Liebsch M, Linscheid M Fahr A, Schäfer-Korting M, Lademann J, Patzelt A (2014) Influence of massage and occlusion on the ex vivo skin penetration of rigid liposomes and invasomes. *Eur J Pharm Biopharm* 86: 301-306.